

Halo-Independent Dark Matter Electron Scattering Analysis with In-Medium Effects

Muping Chen,^{1,*} Graciela B. Gelmini,^{1,†} and Volodymyr Takhistov^{2,3,4,‡}

¹*Department of Physics and Astronomy, UCLA,
475 Portola Plaza, Los Angeles, CA 90095, USA*

²*International Center for Quantum-field Measurement Systems for Studies of the Universe and Particles (QUP, WPI), High Energy Accelerator Research Organization (KEK), Oho 1-1, Tsukuba, Ibaraki 305-0801, Japan*

³*Theory Center, Institute of Particle and Nuclear Studies (IPNS),
High Energy Accelerator Research Organization (KEK), Tsukuba 305-0801, Japan*

⁴*Kavli Institute for the Physics and Mathematics of the Universe (WPI), UTIAS,
The University of Tokyo, Kashiwa, Chiba 277-8583, Japan*

(Dated: September 23, 2022)

Dark matter (DM)-electron scattering is a prime target of a number of direct DM detection experiments and constitutes a promising avenue for exploring interactions of DM in the sub-GeV mass-range, challenging to probe with nuclear recoils. We extend the recently proposed halo-independent analysis method for DM-electron scattering, which allows to infer the local DM halo properties without any additional assumptions about them, to include in-medium effects through dielectric functions of the target material. We show that in-medium effects could significantly affect halo-independent analysis response functions for germanium and silicon and thus are essential for proper inference of local DM halo characteristics from direct DM detection data.

I. INTRODUCTION

The nature of predominant constituent of matter in the Universe, dark matter (DM), remains unknown beyond its gravitational interactions. Numerous proposals have been put forth to explore its possible non-gravitational interactions (see e.g. for review [1, 2]). While significant efforts have focused on studying DM consisting of Weakly Interacting Massive Particles (WIMPs) with typical masses in the GeV to 100 TeV range that often appear in models that can address the hierarchy problem, a wide range of DM candidates covering orders of magnitude in mass-range are feasible. One well motivated possibility is that of DM consisting of light sub-GeV mass particles, which can appear in variety of models (e.g. [3–8]).

Traditional direct detection searches focus on energies deposited from Galactic halo GeV-mass DM interacting with nucleons (see e.g. [9, 10]). Due to kinematics that puts energy deposited in scatterings with nuclei below experimental thresholds, sub-GeV DM interactions with electrons at low-threshold experiments constitutes a preferred paradigm. A broad range of studies have explored DM-electron interactions in experiments based on noble gases and semiconductors, and a slew of experimental search proposals have been put forth (e.g. [11–23]). Already exploited as prime target of experimental collaborations such as XENON1T [24, 25] and XENONnT [26], DAMIC [27], SENSEI [28], and SuperCDMS [29], testing DM-electron interactions is poised to be of importance in future direct DM detection searches [30].

DM-electron scattering in noble gases, like xenon, involve interactions with individual atoms (see e.g. [31]). Crystal targets allow to achieve lower detection thresholds at the level of $\sim \mathcal{O}(1)\text{eV}$ compared $\sim \mathcal{O}(1)\text{keV}$ of noble gases, due to their band structure. However, lattice many-body effects complicate the description of DM-electron interactions in crystals. In Ref. [32, 33] DM-electron scattering in crystals was calculated with semi-analytic approximations for the electron wave functions. Numerical calculations based on density functional theory (DFT) to obtain the crystal band structure and electron wave functions were developed in Ref. [15, 31, 34]. Another approach based on DFT was presented in Ref. [17, 19], subsequently extended to combine DFT with semi-analytic approximations to include a broad range of transition states near and further away from the band gap [35].

Since 1980's [36] conventional direct DM detection analyses focused on assuming a model of the local DM velocity distribution and density, obtaining limits on DM mass-reference cross section ($m_\chi, \sigma_{\text{ref}}$) space for a particular type of DM interaction. On the other hand, halo-independent analyses avoid the uncertainties associated with our knowledge of the local Galactic halo at the small scales relevant for direct detection and allow to instead infer the local DM distribution from signals as well as directly compare results between distinct experiments. While the halo-independent method has been extensively explored for DM-nucleon scattering (see e.g. [37–69]), halo uncertainties can also significantly impact DM-electron searches [70, 71] and only recently Ref. [72] formulated the halo-independent analysis for DM-electron scattering.

Collective in-medium effects in condensed matter systems can significantly modify the DM-electron scattering rates, as first noted for a vector mediator (dark photon) [12] and subsequently for a scalar mediator as

* mpchen@physics.ucla.edu

† gelmini@physics.ucla.edu

‡ vtakhist@post.kek.jp

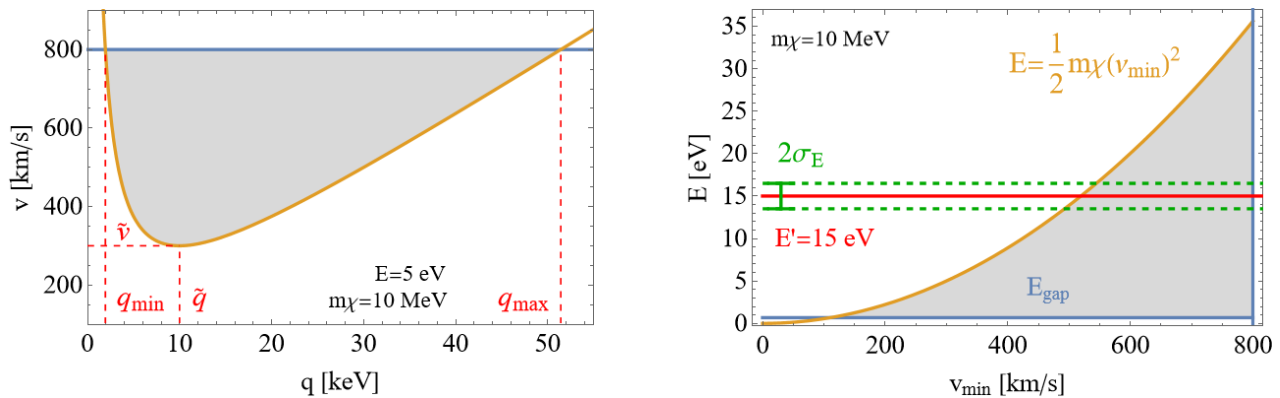


FIG. 1. [Left] Function $v_{\min}(q, E)$ (orange line) for $m_\chi = 10$ MeV and $E = 5$ eV. Indicated are $\tilde{v} = \sqrt{2E/m_\chi}$, The minimum v_{\min} value corresponding to $\tilde{q} = \sqrt{2m_\chi E}$, which separates the left and right q branches, as well as $q_{\min} = q_-(v_{\max}, E)$, and $q_{\max} = q_+(v_{\max}, E)$ are indicated. Here we take the possible maximum DM speed to be $v_{\max} = 800$ km/s, corresponding to DM bound to the Galaxy. The kinematically allowed region is shown in grey. [Right] E integration domain in Eq. (12) (grey region) as function of v_{\min} for $m_\chi = 10$ MeV between the band gap energy (0.67 eV for Ge and 1.1 eV for Si) and the maximum possible recoil energy for a fixed v_{\min} , $E = m_\chi v_{\min}^2/2$. The box resolution function we assume is shown for $E' = 15$ eV and $\sigma_E = 1.5$ eV.

well [73]. These effects could be effectively accounted for through the dielectric function, which is well-studied in a broad range of materials and directly related to the scattering rate [74–76] (see also discussion in [35]).

In this work we build on results of Ref. [72] to formulate the halo-independent DM-electron scattering analysis including in-medium effects, based on the dielectric function.

II. DARK MATTER-ELECTRON SCATTERING

We first provide an overview of the DM-electron scattering rate, including in-medium effects, as employed in conventional direct DM detection analysis (i.e. in a “halo-dependent analysis”).

All the relevant in-medium effects are specified via the dielectric function ϵ , which is experimentally well determined for a broad range of materials, as the energy loss function $\text{Im}[-1/\epsilon(E, \vec{q})]$, where E and \vec{q} are the energy and momentum imparted to the electron. This is incorporated in the dynamic structure factor S that describes the rate of creating density fluctuations in the medium and is related to the longitudinal dielectric response function $\epsilon = \epsilon_L$ via [77]

$$S(E, \vec{q}) = \frac{q^2}{2\pi\alpha} \frac{1}{1 - e^{-\beta E}} \text{Im} \left[\frac{-1}{\epsilon(E, \vec{q})} \right], \quad (1)$$

where $\beta = k_B T$ for temperature T and Boltzmann constant k_B , α is the fine structure constant.

The complete expression for the time average (over a full year) DM-electron scattering event rate, in number of counts per unit time per unit mass, including the structure factor S incorporating in-medium effects through

the dielectric function ϵ , is then given by [76]

$$R = \frac{1}{\rho_T} \frac{\rho_\chi}{m_\chi} \frac{\sigma_{\text{ref}}}{\mu_{\chi e}^2} \frac{\pi}{\alpha} \int d^3 v f_\chi(\vec{v}) \int \frac{d^3 \vec{q}}{(2\pi)^3} q^2 |F_{\text{DM}}(q)|^2 \times \int \frac{dE}{2\pi} \frac{1}{1 - e^{-\beta E}} \text{Im} \left[\frac{-1}{\epsilon(E, \vec{q})} \right] \delta \left(E + \frac{q^2}{2m_\chi} - \vec{q} \cdot \vec{v} \right). \quad (2)$$

Here ρ_χ is the local DM density, ρ_T is the target density, $\mu_{\chi e} = m_\chi m_e / (m_\chi + m_e)$ is the DM-electron reduced mass, $F_{\text{DM}}(q)$ is the DM-mediator form factor, which depends on the mediator mass, and $f_\chi(\vec{v})$ is the time average distribution of DM velocity \vec{v} with respect to the detector, normalized to 1, which in the halo-dependent analysis is typically taken to correspond to that of the Standard Halo Model.

III. HALO-INDEPENDENT ANALYSIS

The halo-independent analysis method is based on separating astrophysical quantities contributing to DM scattering rate from the particle physics and experiment-specific quantities contributing to it. The predicted time average scattering rate can be written in terms of a function $\tilde{\eta}$ characterizing the local DM halo convoluted with a “response function”, a kernel that encodes the detector and particle model information as

$$\frac{dR}{dE}(E) = \int_0^\infty dv_{\min} \tilde{\eta}(v_{\min}) \frac{d\mathcal{R}}{dE}(v_{\min}, E). \quad (3)$$

Here dR/dE is the energy differential average rate (per unit time per unit mass), $d\mathcal{R}/dE$ is the response function

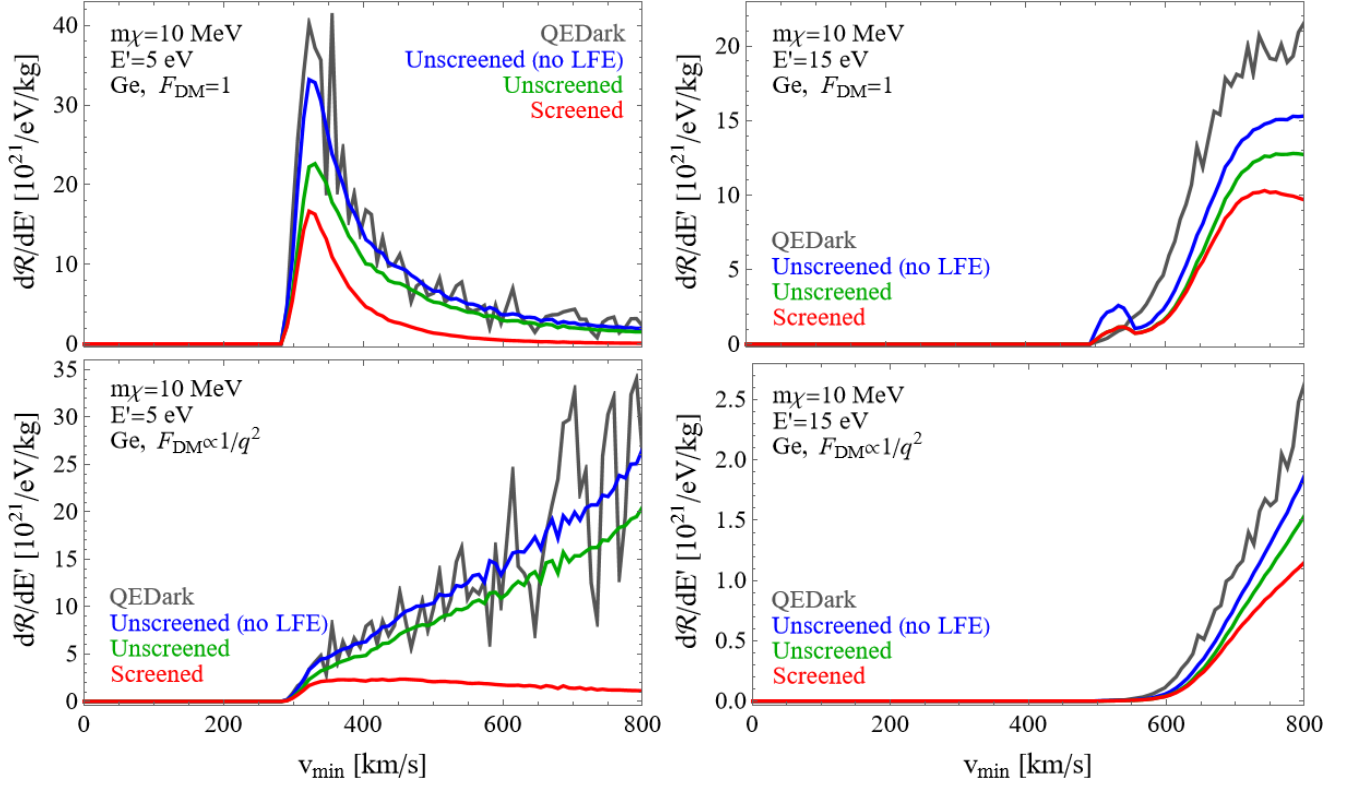


FIG. 2. Response function in germanium for $\tilde{\eta}(v_{\min})$, $d\mathcal{R}(v_{\min}, E')/dE'$, defined in Eq. (11) calculated with different methods: QEDark(gray) and three different approaches in DarkELF, namely unscreened without LFE (blue), unscreened with LFE (green) and screened with LFE (red), for $E' = 5$ eV (left panels) and $E' = 15$ eV (right panels), with DM-mediator form factor $F_{\text{DM}} = 1$ (upper panels) and $F_{\text{DM}} \sim 1/q^2$ (lower panels). Halo properties can be inferred from data only where $d\mathcal{R}/dE' \neq 0$.

for an energy E , and the function

$$\begin{aligned} \tilde{\eta}(v_{\min}) &\equiv \frac{\rho_{\chi}\sigma_{\text{ref}}}{m_{\chi}} \int_{v>v_{\min}} d^3v \frac{f_{\chi}(\vec{v})}{v} \\ &= \frac{\rho_{\chi}\sigma_{\text{ref}}}{m_{\chi}} \int_{v_{\min}}^{\infty} dv \frac{F(v)}{v}, \end{aligned} \quad (4)$$

includes all the DM halo dependence of the rate. Here $F(v) \equiv v^2 \int d\Omega_v f_{\chi}(\vec{v}, t)$ is the speed $v = |\vec{v}|$ distribution. The aim of the halo-independent analysis method is to derive the halo function $\tilde{\eta}$ using direct detection data. Then, data from different direct detection experiments all detecting DM should produce compatible $\tilde{\eta}$ functions.

For DM-electron scattering v_{\min} , the minimum speed of the DM particle necessary to produce a recoil energy E and momentum transfer \vec{q} in a target electron, is

$$v_{\min} = \frac{E}{q} + \frac{q}{2m_{\chi}}. \quad (5)$$

To bring the rate to the form in Eq. (3), we reformulate Eq. (2). Using Eq. (5), we can rewrite the delta-function ensuring energy conservation in Eq. (2) as

$$\delta\left(E + \frac{q^2}{2m_{\chi}} - qv \cos\theta_{qv}\right) = \frac{1}{qv} \delta\left(\cos\theta_{qv} - \frac{v_{\min}}{v}\right). \quad (6)$$

where θ_{qv} is the angle between vectors \vec{q} and \vec{v} . Performing the integration over the solid angle Ω_{qv} we obtain

$$\begin{aligned} R &= \frac{1}{\rho_T} \frac{1}{\mu_{\chi e}^2} \frac{\pi}{\alpha} \frac{1}{(2\pi)^3} \int dq \int dE q^3 |F_{\text{DM}}(q)|^2 \text{Im} \left[\frac{-1}{\epsilon(E, \vec{q})} \right] \\ &\times \frac{1}{1 - e^{-\beta E}} \left[\int d^3v \frac{\rho_{\chi}\sigma_{\text{ref}}}{m_{\chi}} \Theta(v - v_{\min}) \frac{f(\vec{v})}{v} \right], \end{aligned} \quad (7)$$

where Θ is the step function. Notice that the term in the square brackets is $\tilde{\eta}(v_{\min})$ defined in Eq. (4).

Taking the derivative of Eq. (7) with respect to E and performing the change of variables q to v_{\min} , we obtain the desired differential DM-scattering rate in terms of v_{\min} ,

$$\begin{aligned} \frac{dR_{\pm}}{dE} &= \frac{1}{\rho_T} \frac{1}{8\pi^2 \mu_{\chi e}^2 \alpha} \int_0^{v_{\max}} dv_{\min} J_{\pm}(E, v_{\min}) \\ &\times q^3(E, v_{\min}) |F_{\text{DM}}(q(E, v_{\min}))|^2 \\ &\times \frac{1}{1 - e^{-\beta E}} \text{Im} \left[\frac{-1}{\epsilon(E, q(v_{\min}, E))} \right] \tilde{\eta}(v_{\min}), \end{aligned} \quad (8)$$

where $J_{\pm}(E, v_{\min}) = \partial q_{\pm} / \partial v_{\min}$ is the Jacobian due to the change of variables.

For a fixed E , the momentum q has two solutions $q_{\pm}(v_{\min}, E)$ as function of v_{\min} . The two q branches meet

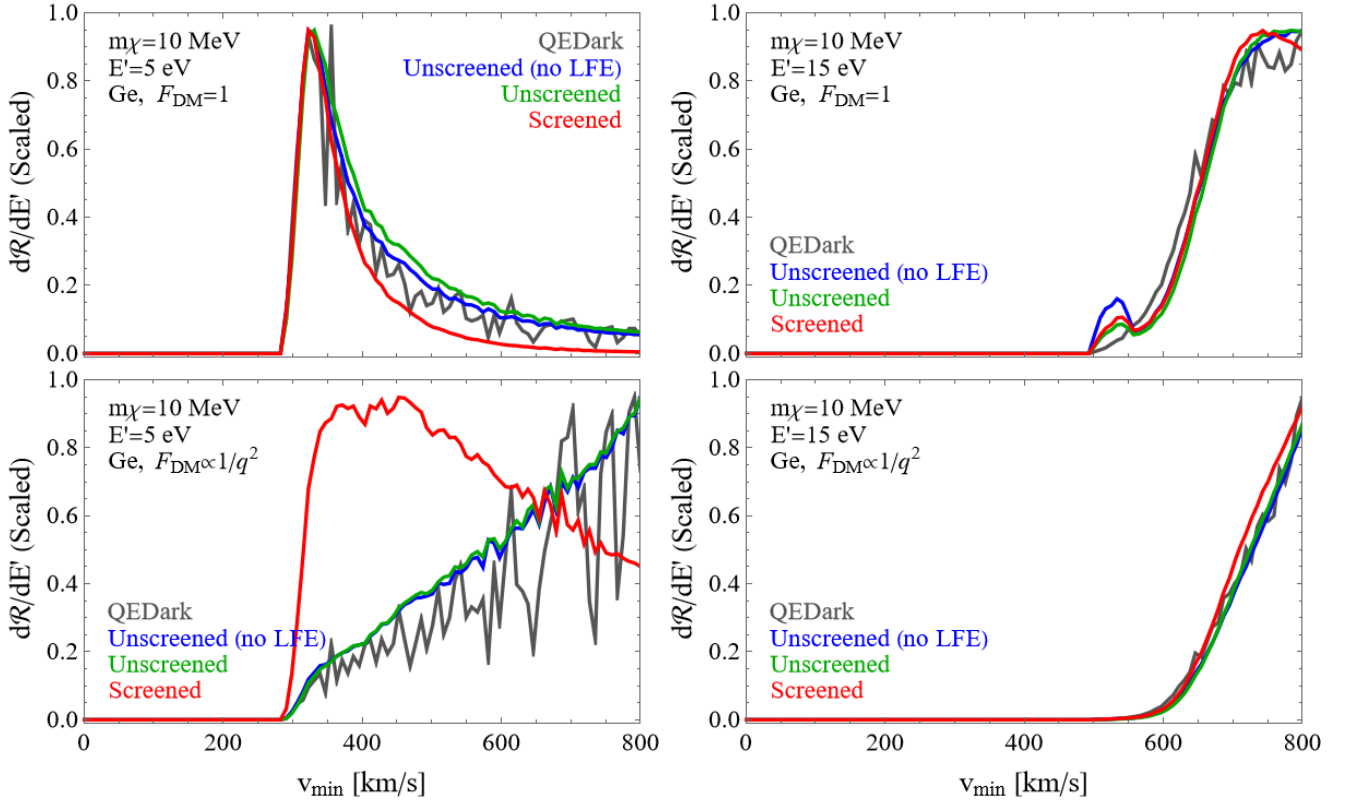


FIG. 3. Same as Fig. 2 but the response functions $d\mathcal{R}/dE'$ are scaled so their maximum is approximately 1, to better show their shape and thus the range of v_{\min} which each allows to explore when interpreted as window functions.

at the minimum v_{\min} value $\tilde{v} = \sqrt{2E/m_\chi}$, where q takes the value $\tilde{q} = q_+(\tilde{v}, E) = q_-(\tilde{v}, E) = \sqrt{2m_\chi E}$, as illustrated in the left panel of Fig. 1. In this figure the blue line horizontal line shows the maximum possible speed v_{\max} of a DM particle in Earth's frame which we take to be $v_{\max} = 800$ km/s. Also indicated are the minimum and maximum values q can take for a given E , $q_{\min} = q_-(v_{\max}, E)$ and $q_{\max} = q_+(v_{\max}, E)$. The possible values of the energy E range from the energy gap $E_{\min} = E_{\text{gap}}$ (0.67 eV for Ge and 1.1 eV for Si) [78, 79], to $E_{\max} = m_\chi v_{\max}^2/2$, the maximum kinetic energy the DM particle can have before scattering.

The total differential rate is then

$$\frac{dR}{dE} = \frac{dR_+}{dE} - \frac{dR_-}{dE}. \quad (9)$$

Here, the differential rate of the left branch, dR_-/dE , carries a negative sign due to the interchange of the lower and the upper limit in the v_{\min} integral in Eq. (8).

Experiments do not directly measure the recoil energy E , but rather a proxy for it that we denote E' such as some amount of heat or a number of photoelectrons. We account for this by relating the true differential recoil rate dR/dE to the detected differential recoil rate dR/dE' as

$$\frac{dR}{dE'} = \varepsilon(E') \int_0^\infty dE G(E', E) \frac{dR}{dE}, \quad (10)$$

where the $\varepsilon(E')$ function accounts for the detector efficiency and $G(E', E)$ is the energy resolution function of the experiment. For simplicity, for our figures we assume a box resolution function with width $2\sigma_E$ centered at E' and $\sigma_E = 0.1E'$.

Combining Eq. (8), Eq. (9), and Eq. (10), we obtain the halo-independent analysis response function $d\mathcal{R}/dE'$, defined in Eq. (3) by replacing E by E' , as

$$\frac{d\mathcal{R}}{dE'}(E', v_{\min}) = \frac{d\mathcal{R}_+}{dE'} - \frac{d\mathcal{R}_-}{dE'} \quad (11)$$

where

$$\begin{aligned} \frac{d\mathcal{R}_\pm}{dE'}(E', v_{\min}) &= \frac{1}{\rho_T} \frac{\varepsilon(E')}{8\pi^2 \mu_{\chi e}^2 \alpha} \int dE G(E', E) \quad (12) \\ &\times J_\pm(E, v_{\min}) q_\pm^3(E, v_{\min}) |F_{\text{DM}}(q_\pm(E, v_{\min}))|^2 \\ &\times \frac{1}{1 - e^{-\beta E}} \text{Im} \left[\frac{-1}{\epsilon(E, q_\pm(v_{\min}, E))} \right]. \end{aligned}$$

IV. COMPUTATION METHOD

The computation of the response function in Eq. (11), requires specifying the integration domain, the energy resolution function, the DM-mediator form factor, and the dielectric function of the specific material.

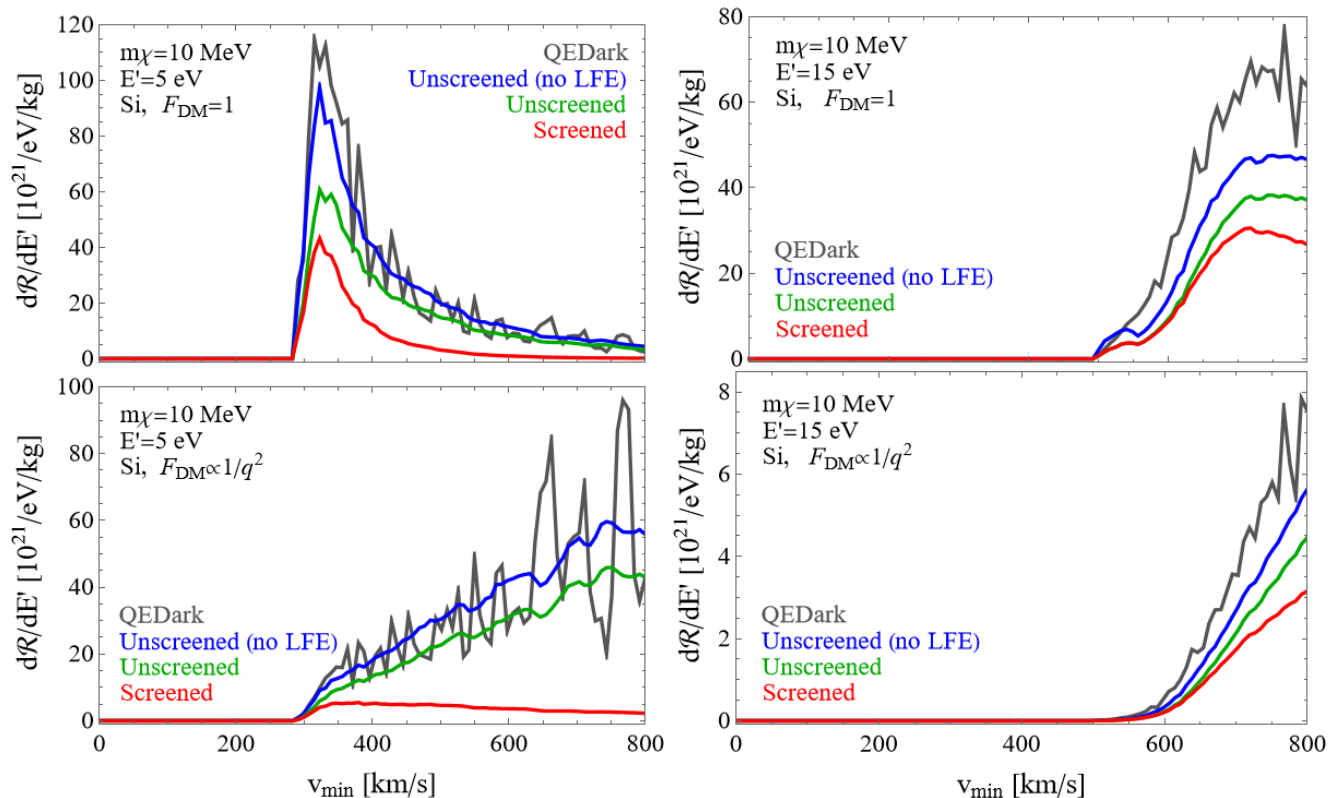


FIG. 4. Same as Fig. 2 but for silicon.

The right panel of Fig. (1) shows the integration domain in E for each fixed v_{\min} value. It goes between E_{gap} and $E = m_{\chi} v_{\min}^2/2$ (shown as the yellow curve in Fig. (1)), the maximum possible recoil energy due to a collision of a DM particle moving with speed v_{\min} (we can see this corresponds to inverting the function $\tilde{v}(E)$ when taking $\tilde{v} = v_{\min}$). As we have mentioned, for simplicity, we assume a simple box distribution for the energy resolution. The results are very similar when using a more realistic distribution, such as Gaussian.

For our figures we chose $m_{\chi} = 10$ MeV, in which case E' can go between 0.67 eV and 35.6 eV (when $v_{\min} = 800$ km/s). For our plots we choose two representative values, $E' = 5$ eV (considering that detecting at least one electron requires 2.9 eV in Ge and 3.6 eV in Si [34]), and $E' = 15$ eV.

We consider two DM-mediator form factors, $F_{\text{DM}} = 1$ for a heavy mediator and $F_{\text{DM}} = (\alpha m_e/q)^2$ for a light mediator, which generally appear in a variety of models such as the scenarios of vector-portal DM with a dark photon mediator or magnetic-dipole-moment interactions.

For the dielectric function, we employ the output data from DarkELF [76] and interpolate it into a continuous function. The dielectric function data are calculated using GPAW [80, 81] that relies on first principles time-dependent DFT. DarkELF allows the calculation to be carried out with or without considering screening and local field effects (LFE) (i.e. including or excluding infor-

mation on the non-diagonal components of the dielectric matrix). In our Figs. 2 and 3 we show results the following cases: 1) with screening and with LFE (red lines); 2) without screening effect (namely $|\epsilon|^2 = 1$) but with LFE (green lines); 3) without screening effect or LFE (blue lines). We also compare results from these three cases to results of QEDark [34] (dark grey lines), as obtained in our previous paper [72].

It is worth noting that the maximum value of q for the DarkELF data is 22.5 keV while it is approximately 67 keV for QEDark. To compare the models for the same parameters range, we use $q_{\text{cut}} = 22.5$ keV for all our computations. For $E' = 5$ eV, we have $q_{\min}(E = 4.5 \text{ eV}) = 1.7 \text{ keV}$, $q_{\max}(E = 4.5 \text{ eV}) = 51.6 \text{ keV}$, and maximum $\tilde{q}(E = 5.5 \text{ eV}) = 10.5 \text{ keV}$. For $E' = 15$ eV, $q_{\min}(E = 13.5 \text{ eV}) = 5.7 \text{ keV}$, $q_{\max}(E = 13.5 \text{ eV}) = 47.7 \text{ keV}$, and maximum $\tilde{q}(E = 16.5 \text{ eV}) = 18.2 \text{ keV}$. We can see that for the two representative energy values, we get the whole left branch and part of the right branch with this choice of momentum cut. The whole integral is then numerically evaluated over the range discussed above using Mathematica.

V. RESULTS

Figs. 2 and 3 show the response functions $d\mathcal{R}/dE'$ as a function of v_{\min} in Ge, calculated with three different

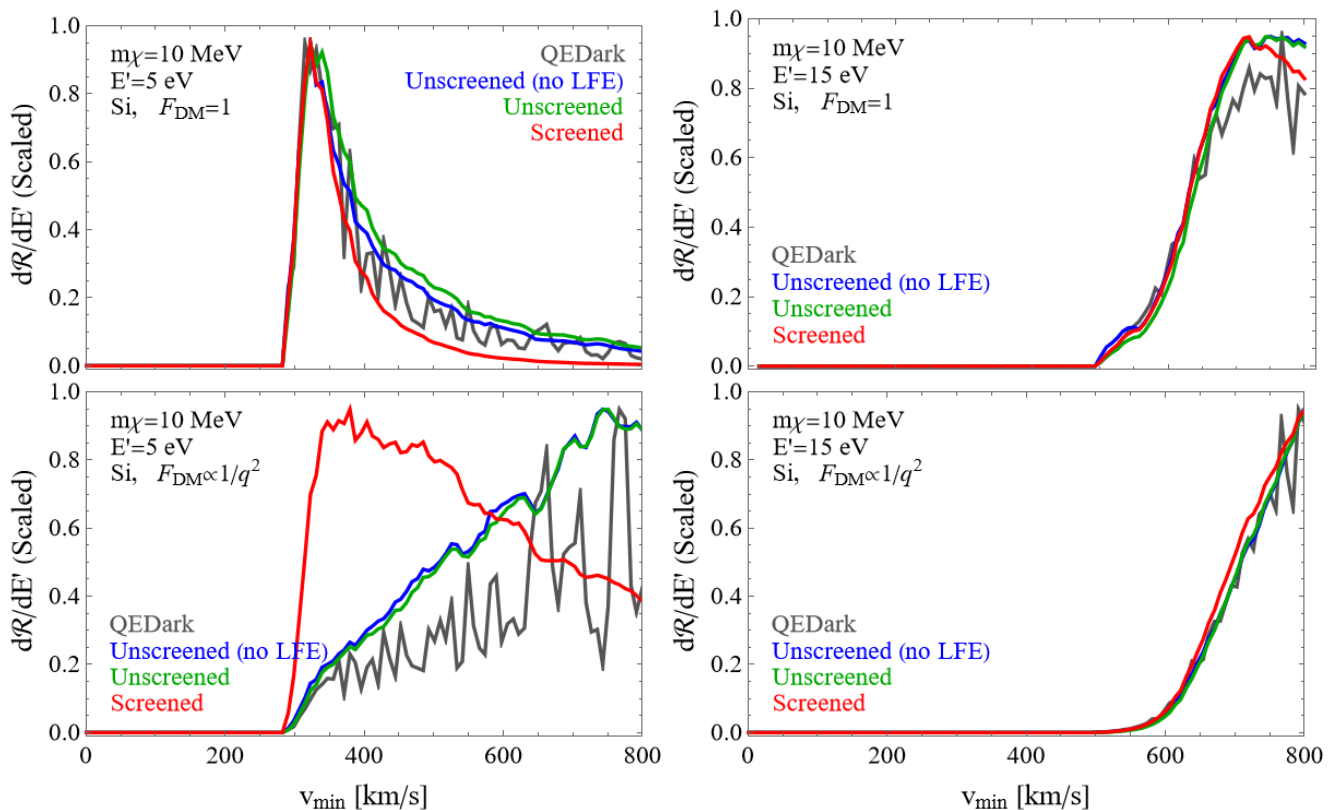


FIG. 5. Same as Fig. 3 but for silicon.

dielectric function computation methods using DarkELF, and additionally with QEDark. We find that the results for Si are very similar. They are shown in Figs. 4 and 5.

The plots are made with 100 v_{\min} values, chosen with equal spacing over the domain (0, 800) km/s. These figures show the response functions for detected energy $E' = 5$ eV (left panels) and $E' = 15$ eV (right panels), and two different DM form factors $F_{\text{DM}} = 1$ (upper panels) and $F_{\text{DM}} = (\alpha m_e 1/q)^2$ (lower panels).

In Figs. 2 and 4, the response functions are plotted in their original natural units. In Figs. 3 and 5 the response functions are instead scaled so that the maximum of each curve is close to 1 (which is the way the QEDark results were shown in Ref. [72]). Recall that the response function acts as a window function through which measured rates in direct detection experiments can provide information about the DM velocity (or speed) distribution through the function $\tilde{\eta}(v_{\min})$. By scaling the response functions we can better appreciate the range of v_{\min} selected by each of them.

In Fig. 2 and 4 we see that the QEDark results (dark grey lines) in general are similar to the results using the unscreened without LFE GPAW calculation (blue lines), the unscreened with LFE GPAW calculation (green lines) is intermediate between the previous two and the result using the screened with LFE GPAW calculation (red lines). This is roughly in agreement with the results shown in Fig. 5 of Ref. [75] for upper limits on σ_{ref}

as function of m_χ for the four different models. There too the QEDark results are similar with the unscreened without LFE limits and they the least restrictive, the unscreened with LFE limits are intermediate and the most restrictive limits are those of the screened with LFE GPAW calculation.

We can also see that the screening effect effectively reduce the amplitude of the response function, and this effect is much more pronounced for $F_{\text{DM}} \sim 1/q^2$, especially in the low E' regime.

The weight assigned by the response functions calculated in different cases as window function to different values of v_{\min} are in general very similar, as we can see in Figs. 3 and 5. However, the shape of the window function can change considerably in the regime where the screening effect is much more pronounced, as shown in the lower left panel of Fig. 3 and 5.

VI. CONCLUSIONS

Light sub-GeV DM constitutes a promising target for exploration in direct DM detection experiments studying DM-electron scattering. While conventional direct DM detection analysis depends on assumptions about poorly known local halo DM distribution, the halo-independent analysis allows to infer local DM halo properties from direct detection data and consistently analyze distinct

experimental targets. In crystal target materials, which allow achieving lower experimental thresholds, collective in-medium effects could modify signatures of DM interactions. Here we formulate for the first time the methodology for halo-independent direct DM detection analysis for DM-electron scattering including in-medium effects. We show for a germanium target, and similarly for a silicon target, that in-medium effects could significantly impact the interpretation of direct DM detection data. Thus, such effects must be included in future halo-independent analyses for proper inference of local DM halo properties

from DM detection data.

ACKNOWLEDGMENTS

We thank Tongyan Lin for comments and Tien-Tien Yu for discussions and clarifications regarding the QEdark package. The work of G.B.G. and M.C. was supported in part by the U.S. Department of Energy (DOE) Grant No. DE-SC0009937. V.T. was also supported by the World Premier International Research Center Initiative (WPI), MEXT, Japan.

-
- [1] Gianfranco Bertone, Dan Hooper, and Joseph Silk, “Particle dark matter: Evidence, candidates and constraints,” *Phys. Rept.* **405**, 279–390 (2005), arXiv:hep-ph/0404175.
- [2] Graciela B. Gelmini, “The Hunt for Dark Matter,” in *Theoretical Advanced Study Institute in Elementary Particle Physics: Journeys Through the Precision Frontier: Amplitudes for Colliders* (2015) pp. 559–616, arXiv:1502.01320 [hep-ph].
- [3] Jonathan L. Feng and Jason Kumar, “The WIMP-less Miracle: Dark-Matter Particles without Weak-Scale Masses or Weak Interactions,” *Phys. Rev. Lett.* **101**, 231301 (2008), arXiv:0803.4196 [hep-ph].
- [4] C. Boehm and Pierre Fayet, “Scalar dark matter candidates,” *Nucl. Phys. B* **683**, 219–263 (2004), arXiv:hep-ph/0305261.
- [5] Tongyan Lin, Hai-Bo Yu, and Kathryn M. Zurek, “On Symmetric and Asymmetric Light Dark Matter,” *Phys. Rev. D* **85**, 063503 (2012), arXiv:1111.0293 [hep-ph].
- [6] Dan Hooper and Kathryn M. Zurek, “A Natural Supersymmetric Model with MeV Dark Matter,” *Phys. Rev. D* **77**, 087302 (2008), arXiv:0801.3686 [hep-ph].
- [7] Yonit Hochberg, Eric Kuflik, Tomer Volansky, and Jay G. Wacker, “Mechanism for Thermal Relic Dark Matter of Strongly Interacting Massive Particles,” *Phys. Rev. Lett.* **113**, 171301 (2014), arXiv:1402.5143 [hep-ph].
- [8] Yonit Hochberg, Eric Kuflik, Hitoshi Murayama, Tomer Volansky, and Jay G. Wacker, “Model for Thermal Relic Dark Matter of Strongly Interacting Massive Particles,” *Phys. Rev. Lett.* **115**, 021301 (2015), arXiv:1411.3727 [hep-ph].
- [9] Graciela B. Gelmini, Volodymyr Takhistov, and Samuel J. Witte, “Casting a Wide Signal Net with Future Direct Dark Matter Detection Experiments,” *JCAP* **07**, 009 (2018), [Erratum: *JCAP* **02**, E02 (2019)], arXiv:1804.01638 [hep-ph].
- [10] D. S. Akerib *et al.*, “Snowmass2021 Cosmic Frontier Dark Matter Direct Detection to the Neutrino Fog,” in *2022 Snowmass Summer Study* (2022) arXiv:2203.08084 [hep-ex].
- [11] Yonit Hochberg, Yue Zhao, and Kathryn M. Zurek, “Superconducting Detectors for Superlight Dark Matter,” *Phys. Rev. Lett.* **116**, 011301 (2016), arXiv:1504.07237 [hep-ph].
- [12] Yonit Hochberg, Matt Pyle, Yue Zhao, and Kathryn M. Zurek, “Detecting Superlight Dark Matter with Fermi-Degenerate Materials,” *JHEP* **08**, 057 (2016), arXiv:1512.04533 [hep-ph].
- [13] Yonit Hochberg, Yonatan Kahn, Mariangela Lisanti, Christopher G. Tully, and Kathryn M. Zurek, “Directional detection of dark matter with two-dimensional targets,” *Phys. Lett. B* **772**, 239–246 (2017), arXiv:1606.08849 [hep-ph].
- [14] Yonit Hochberg, Yonatan Kahn, Mariangela Lisanti, Kathryn M. Zurek, Adolfo G. Grushin, Roni Ilan, Sinéad M. Griffin, Zhen-Fei Liu, Sophie F. Weber, and Jeffrey B. Neaton, “Detection of sub-MeV Dark Matter with Three-Dimensional Dirac Materials,” *Phys. Rev. D* **97**, 015004 (2018), arXiv:1708.08929 [hep-ph].
- [15] Stephen Derenzo, Rouven Essig, Andrea Massari, Adrian Soto, and Tien-Tien Yu, “Direct Detection of sub-GeV Dark Matter with Scintillating Targets,” *Phys. Rev. D* **96**, 016026 (2017), arXiv:1607.01009 [hep-ph].
- [16] Noah Alexander Kurinsky, To Chin Yu, Yonit Hochberg, and Blas Cabrera, “Diamond Detectors for Direct Detection of Sub-GeV Dark Matter,” *Phys. Rev. D* **99**, 123005 (2019), arXiv:1901.07569 [hep-ex].
- [17] Sinéad M. Griffin, Katherine Inzani, Tanner Trickle, Zhengkang Zhang, and Kathryn M. Zurek, “Multichannel direct detection of light dark matter: Target comparison,” *Phys. Rev. D* **101**, 055004 (2020), arXiv:1910.10716 [hep-ph].
- [18] Carlos Blanco, J. I. Collar, Yonatan Kahn, and Benjamin Lillard, “Dark Matter-Electron Scattering from Aromatic Organic Targets,” *Phys. Rev. D* **101**, 056001 (2020), arXiv:1912.02822 [hep-ph].
- [19] Tanner Trickle, Zhengkang Zhang, Kathryn M. Zurek, Katherine Inzani, and Sinéad Griffin, “Multi-Channel Direct Detection of Light Dark Matter: Theoretical Framework,” *JHEP* **03**, 036 (2020), arXiv:1910.08092 [hep-ph].
- [20] R. Matthias Geilhufe, Felix Kahlhoefer, and Martin Wolfgang Winkler, “Dirac Materials for Sub-MeV Dark Matter Detection: New Targets and Improved Formalism,” *Phys. Rev. D* **101**, 055005 (2020), arXiv:1910.02091 [hep-ph].
- [21] Yonit Hochberg, Ilya Charaev, Sae-Woo Nam, Varun Verma, Marco Colangelo, and Karl K. Berggren, “Detecting Sub-GeV Dark Matter with Superconducting Nanowires,” *Phys. Rev. Lett.* **123**, 151802 (2019), arXiv:1903.05101 [hep-ph].
- [22] Ahmet Coskuner, Andrea Mitridate, Andres Olivares, and Kathryn M. Zurek, “Directional Dark Matter Detection in Anisotropic Dirac Materials,” *Phys. Rev. D* **103**, 016006 (2021), arXiv:1909.09170 [hep-ph].

- [23] Sinéad M. Griffin, Yonit Hochberg, Katherine Inzani, Noah Kurinsky, Tongyan Lin, and To Chin, “Silicon carbide detectors for sub-GeV dark matter,” *Phys. Rev. D* **103**, 075002 (2021), arXiv:2008.08560 [hep-ph].
- [24] E. Aprile *et al.* (XENON), “Light Dark Matter Search with Ionization Signals in XENON1T,” *Phys. Rev. Lett.* **123**, 251801 (2019), arXiv:1907.11485 [hep-ex].
- [25] E. Aprile *et al.* (XENON), “Excess electronic recoil events in XENON1T,” *Phys. Rev. D* **102**, 072004 (2020), arXiv:2006.09721 [hep-ex].
- [26] E. Aprile *et al.*, “Search for New Physics in Electronic Recoil Data from XENONnT,” (2022), arXiv:2207.11330 [hep-ex].
- [27] A. Aguilar-Arevalo *et al.* (DAMIC), “Constraints on Light Dark Matter Particles Interacting with Electrons from DAMIC at SNOLAB,” *Phys. Rev. Lett.* **123**, 181802 (2019), arXiv:1907.12628 [astro-ph.CO].
- [28] Liron Barak *et al.* (SENSEI), “SENSEI: Direct-Detection Results on sub-GeV Dark Matter from a New Skipper-CCD,” *Phys. Rev. Lett.* **125**, 171802 (2020), arXiv:2004.11378 [astro-ph.CO].
- [29] D. W. Amaral *et al.* (SuperCDMS), “Constraints on low-mass, relic dark matter candidates from a surface-operated SuperCDMS single-charge sensitive detector,” *Phys. Rev. D* **102**, 091101 (2020), arXiv:2005.14067 [hep-ex].
- [30] Rouven Essig, Graham K. Giovanetti, Noah Kurinsky, Dan McKinsey, Karthik Ramanathan, Kelly Stifter, and Tien-Tien Yu, “Snowmass2021 Cosmic Frontier: The landscape of low-threshold dark matter direct detection in the next decade,” in *2022 Snowmass Summer Study* (2022) arXiv:2203.08297 [hep-ph].
- [31] Rouven Essig, Jeremy Mardon, and Tomer Volansky, “Direct Detection of Sub-GeV Dark Matter,” *Phys. Rev. D* **85**, 076007 (2012), arXiv:1108.5383 [hep-ph].
- [32] Peter W. Graham, David E. Kaplan, Surjeet Rajendran, and Matthew T. Walters, “Semiconductor Probes of Light Dark Matter,” *Phys. Dark Univ.* **1**, 32–49 (2012), arXiv:1203.2531 [hep-ph].
- [33] Samuel K. Lee, Mariangela Lisanti, Siddharth Mishra-Sharma, and Benjamin R. Safdi, “Modulation Effects in Dark Matter-Electron Scattering Experiments,” *Phys. Rev. D* **92**, 083517 (2015), arXiv:1508.07361 [hep-ph].
- [34] Rouven Essig, Marivi Fernandez-Serra, Jeremy Mardon, Adrian Soto, Tomer Volansky, and Tien-Tien Yu, “Direct Detection of sub-GeV Dark Matter with Semiconductor Targets,” *JHEP* **05**, 046 (2016), arXiv:1509.01598 [hep-ph].
- [35] Sinéad M. Griffin, Katherine Inzani, Tanner Trickle, Zhengkang Zhang, and Kathryn M. Zurek, “Extended Calculation of Dark Matter-Electron Scattering in Crystal Targets,” (2021), arXiv:2105.05253 [hep-ph].
- [36] S. P. Ahlen, F. T. Avignone, R. L. Brodzinski, A. K. Drukier, G. Gelmini, and D. N. Spergel, “Limits on Cold Dark Matter Candidates from an Ultralow Background Germanium Spectrometer,” *Phys. Lett. B* **195**, 603–608 (1987).
- [37] Patrick J. Fox, Jia Liu, and Neal Weiner, “Integrating Out Astrophysical Uncertainties,” *Phys. Rev. D* **83**, 103514 (2011), arXiv:1011.1915 [hep-ph].
- [38] Patrick J. Fox, Graham D. Kribs, and Tim M. P. Tait, “Interpreting Dark Matter Direct Detection Independently of the Local Velocity and Density Distribution,” *Phys. Rev. D* **83**, 034007 (2011), arXiv:1011.1910 [hep-ph].
- [39] Mads T. Frandsen, Felix Kahlhoefer, Christopher McCabe, Subir Sarkar, and Kai Schmidt-Hoberg, “Resolving astrophysical uncertainties in dark matter direct detection,” *JCAP* **01**, 024 (2012), arXiv:1111.0292 [hep-ph].
- [40] Paolo Gondolo and Graciela B. Gelmini, “Halo independent comparison of direct dark matter detection data,” *JCAP* **12**, 015 (2012), arXiv:1202.6359 [hep-ph].
- [41] Juan Herrero-Garcia, Thomas Schwetz, and Jure Zupan, “Astrophysics independent bounds on the annual modulation of dark matter signals,” *Phys. Rev. Lett.* **109**, 141301 (2012), arXiv:1205.0134 [hep-ph].
- [42] Mads T. Frandsen, Felix Kahlhoefer, Christopher McCabe, Subir Sarkar, and Kai Schmidt-Hoberg, “The unbearable lightness of being: CDMS versus XENON,” *JCAP* **07**, 023 (2013), arXiv:1304.6066 [hep-ph].
- [43] Eugenio Del Nobile, Graciela B. Gelmini, Paolo Gondolo, and Ji-Haeng Huh, “Halo-independent analysis of direct detection data for light WIMPs,” *JCAP* **10**, 026 (2013), arXiv:1304.6183 [hep-ph].
- [44] Nassim Bozorgnia, Juan Herrero-Garcia, Thomas Schwetz, and Jure Zupan, “Halo-independent methods for inelastic dark matter scattering,” *JCAP* **07**, 049 (2013), arXiv:1305.3575 [hep-ph].
- [45] Eugenio Del Nobile, Graciela B. Gelmini, Paolo Gondolo, and Ji-Haeng Huh, “Generalized Halo Independent Comparison of Direct Dark Matter Detection Data,” *JCAP* **10**, 048 (2013), arXiv:1306.5273 [hep-ph].
- [46] Eugenio Del Nobile, Graciela B. Gelmini, Paolo Gondolo, and Ji-Haeng Huh, “Update on Light WIMP Limits: LUX, lite and Light,” *JCAP* **03**, 014 (2014), arXiv:1311.4247 [hep-ph].
- [47] Eugenio Del Nobile, Graciela B. Gelmini, Paolo Gondolo, and Ji-Haeng Huh, “Direct detection of Light Anapole and Magnetic Dipole DM,” *JCAP* **06**, 002 (2014), arXiv:1401.4508 [hep-ph].
- [48] Brian Feldstein and Felix Kahlhoefer, “A new halo-independent approach to dark matter direct detection analysis,” *JCAP* **08**, 065 (2014), arXiv:1403.4606 [hep-ph].
- [49] Patrick J. Fox, Yonatan Kahn, and Matthew McCullough, “Taking Halo-Independent Dark Matter Methods Out of the Bin,” *JCAP* **10**, 076 (2014), arXiv:1403.6830 [hep-ph].
- [50] Graciela B. Gelmini, Andreea Georgescu, and Ji-Haeng Huh, “Direct detection of light Ge-ophobic exothermic dark matter,” *JCAP* **07**, 028 (2014), arXiv:1404.7484 [hep-ph].
- [51] John F. Cherry, Mads T. Frandsen, and Ian M. Shoemaker, “Halo Independent Direct Detection of Momentum-Dependent Dark Matter,” *JCAP* **10**, 022 (2014), arXiv:1405.1420 [hep-ph].
- [52] Eugenio Del Nobile, Graciela B. Gelmini, Paolo Gondolo, and Ji-Haeng Huh, “Update on the Halo-Independent Comparison of Direct Dark Matter Detection Data,” *Phys. Procedia* **61**, 45–54 (2015), arXiv:1405.5582 [hep-ph].
- [53] Stefano Scopel and KookHyun Yoon, “A systematic halo-independent analysis of direct detection data within the framework of Inelastic Dark Matter,” *JCAP* **08**, 060 (2014), arXiv:1405.0364 [astro-ph.CO].
- [54] Brian Feldstein and Felix Kahlhoefer, “Quantifying (dis)agreement between direct detection experiments in a halo-independent way,” *JCAP* **12**, 052 (2014),

- arXiv:1409.5446 [hep-ph].
- [55] Nassim Bozorgnia and Thomas Schwetz, “What is the probability that direct detection experiments have observed Dark Matter?” *JCAP* **12**, 015 (2014), arXiv:1410.6160 [astro-ph.CO].
- [56] Mattias Blennow, Juan Herrero-Garcia, and Thomas Schwetz, “A halo-independent lower bound on the dark matter capture rate in the Sun from a direct detection signal,” *JCAP* **05**, 036 (2015), arXiv:1502.03342 [hep-ph].
- [57] Eugenio Del Nobile, Graciela B. Gelmini, Andreea Georgescu, and Ji-Haeng Huh, “Reevaluation of spin-dependent WIMP-proton interactions as an explanation of the DAMA data,” *JCAP* **08**, 046 (2015), arXiv:1502.07682 [hep-ph].
- [58] Adam J. Anderson, Patrick J. Fox, Yonatan Kahn, and Matthew McCullough, “Halo-Independent Direct Detection Analyses Without Mass Assumptions,” *JCAP* **10**, 012 (2015), arXiv:1504.03333 [hep-ph].
- [59] Mattias Blennow, Juan Herrero-Garcia, Thomas Schwetz, and Stefan Vogl, “Halo-independent tests of dark matter direct detection signals: local DM density, LHC, and thermal freeze-out,” *JCAP* **08**, 039 (2015), arXiv:1505.05710 [hep-ph].
- [60] Stefano Scopel, Kook-Hyun Yoon, and Jong-Hyun Yoon, “Generalized spin-dependent WIMP-nucleus interactions and the DAMA modulation effect,” *JCAP* **07**, 041 (2015), arXiv:1505.01926 [astro-ph.CO].
- [61] Francesc Ferrer, Alejandro Ibarra, and Sebastian Wild, “A novel approach to derive halo-independent limits on dark matter properties,” *JCAP* **09**, 052 (2015), arXiv:1506.03386 [hep-ph].
- [62] Sebastian Wild, Francesc Ferrer, and Alejandro Ibarra, “Halo-independent upper limits on the dark matter scattering cross section with nucleons,” *J. Phys. Conf. Ser.* **718**, 042063 (2016).
- [63] Graciela B. Gelmini, Andreea Georgescu, Paolo Gondolo, and Ji-Haeng Huh, “Extended Maximum Likelihood Halo-independent Analysis of Dark Matter Direct Detection Data,” *JCAP* **11**, 038 (2015), arXiv:1507.03902 [hep-ph].
- [64] Graciela B. Gelmini, Ji-Haeng Huh, and Samuel J. Witte, “Assessing Compatibility of Direct Detection Data: Halo-Independent Global Likelihood Analyses,” *JCAP* **10**, 029 (2016), arXiv:1607.02445 [hep-ph].
- [65] Samuel J. Witte and Graciela B. Gelmini, “Updated Constraints on the Dark Matter Interpretation of CDMS-II-Si Data,” *JCAP* **05**, 026 (2017), arXiv:1703.06892 [hep-ph].
- [66] Paolo Gondolo and Stefano Scopel, “Halo-independent determination of the unmodulated WIMP signal in DAMA: the isotropic case,” *JCAP* **09**, 032 (2017), arXiv:1703.08942 [hep-ph].
- [67] Alejandro Ibarra and Andreas Rappelt, “Optimized velocity distributions for direct dark matter detection,” *JCAP* **08**, 039 (2017), arXiv:1703.09168 [hep-ph].
- [68] Graciela B. Gelmini, Ji-Haeng Huh, and Samuel J. Witte, “Unified Halo-Independent Formalism From Convex Hulls for Direct Dark Matter Searches,” *JCAP* **12**, 039 (2017), arXiv:1707.07019 [hep-ph].
- [69] Riccardo Catena, Alejandro Ibarra, Andreas Rappelt, and Sebastian Wild, “Halo-independent comparison of direct detection experiments in the effective theory of dark matter-nucleon interactions,” *JCAP* **07**, 028 (2018), arXiv:1801.08466 [hep-ph].
- [70] Tarak Nath Maity, Tirtha Sankar Ray, and Sambo Sarkar, “Halo uncertainties in electron recoil events at direct detection experiments,” (2020), arXiv:2011.12896 [hep-ph].
- [71] Aria Radick, Anna-Maria Taki, and Tien-Tien Yu, “Dependence of Dark Matter - Electron Scattering on the Galactic Dark Matter Velocity Distribution,” *JCAP* **02**, 004 (2021), arXiv:2011.02493 [hep-ph].
- [72] Muping Chen, Graciela B. Gelmini, and Volodymyr Takhistov, “Halo-independent analysis of direct dark matter detection through electron scattering,” *JCAP* **12**, 048 (2021), arXiv:2105.08101 [hep-ph].
- [73] Graciela B. Gelmini, Volodymyr Takhistov, and Edoardo Vitagliano, “Scalar direct detection: In-medium effects,” *Phys. Lett. B* **809**, 135779 (2020), arXiv:2006.13909 [hep-ph].
- [74] Yonit Hochberg, Yonatan Kahn, Noah Kurinsky, Benjamin V. Lehmann, To Chin Yu, and Karl K. Berggren, “Determining Dark-Matter-Electron Scattering Rates from the Dielectric Function,” *Phys. Rev. Lett.* **127**, 151802 (2021), arXiv:2101.08263 [hep-ph].
- [75] Simon Knapen, Jonathan Kozaczuk, and Tongyan Lin, “Dark matter-electron scattering in dielectrics,” *Phys. Rev. D* **104**, 015031 (2021), arXiv:2101.08275 [hep-ph].
- [76] Simon Knapen, Jonathan Kozaczuk, and Tongyan Lin, “python package for dark matter scattering in dielectric targets,” *Phys. Rev. D* **105**, 015014 (2022), arXiv:2104.12786 [hep-ph].
- [77] Philip Phillips, *Advanced Solid State Physics*, 2nd ed. (Cambridge University Press, 2012).
- [78] Ben G. Streetman and Sanjay K. Banerjee, *Solid State Electronic Devices* (Prentice Hall, 2005).
- [79] Claude A. Klein, “Bandgap Dependence and Related Features of Radiation Ionization Energies in Semiconductors,” *Journal of Applied Physics* **39**, 2029–2038 (1968).
- [80] J. J. Mortensen, L. B. Hansen, and K. W. Jacobsen, “Real-space grid implementation of the projector augmented wave method,” *Phys. Rev. B* **71**, 035109 (2005), arXiv:cond-mat/0411218 [cond-mat.mtrl-sci].
- [81] J. Enkovaara *et al.*, “Electronic structure calculations with GPAW: a real-space implementation of the projector augmented-wave method,” *Journal of Physics: Condensed Matter* **22**, 253202 (2010).